JOURNAL OF MATERIALS SCIENCE 23 (1988) 451–458

Kinetic study of haematite reduction by hydrogen

N. G. GALLEGOS*, M. A. APECETCHE†
Centro de Investigación y Desarrollo en Procesos Catalíticos (CINDECA), Calle 47 no. 257 (1900) La Plata, Argentina

The reduction of powdered haematite (α-Fe_2O_3) with hydrogen was studied in a fixed-bed differential reactor, in the temperature range 968 to 1063 K under different hydrogen partial pressures, ranging between 0.1 and 0.7 atm. The kinetic parameters were calculated from the measurement of the thermal conductivity variation in the gaseous phase produced by the reaction. The reaction was first order with respect to the hydrogen concentration. In the 968 to 1008 K temperature range, the reaction was chemically controlled and the preexponential factor and the activation energy values obtained were 9.96×10^4 and 40.2 ± 1.6 kcal mol^{-1}, respectively. Beyond 1008 K a retarded reduction was observed indicating that a combined process of direct gas–solid reaction and iron-ion diffusion in the solid occurred.

Nomenclature

A	Area under the kinetic curve (cm^2)
C	Molar concentration (gmol cm^{-3})
$D_{H_2-N_2}$	Diffusivity of hydrogen in the H_2–N_2 mixture (cm^2 min^{-1})
d_p	Particle diameter (nm)
F_v	Total volumetric flow (cm^3 min^{-1})
F_H	Molar flow of hydrogen in reference branch of the detector (gmol min^{-1})
F_N	Molar flow of N_2 in reference branch of the detector (gmol min^{-1})
F_R	Molar flow of H_2 which disappears by reaction (gmol min^{-1})
f_{DT}	Constant factor defined in Equation 7 (mV)
f_e	Recorder signal factor (mV/cm)
k_s	Reaction rate coefficient per unit surface area (cm min^{-1})
m	Reactant solid mass (g)
N_H	Number of moles of reactant gas which react with unit mass of solid reactant (gmol g^{-1})
L	Gas film (nm)
p	Partial pressure (g cm^{-1} min^{-2})
R_g	Gas constant (g cm^2 min^{-2} K^{-1} mol^{-1})
R	Particle radius (nm)
r_v	Reaction rate per unit volume of reactant solid (gmol cm^{-3} min^{-1})
r_M	Slope of solid reactant conversion against time curve (min^{-1})
r_S	Reaction rate (g mol cm^{-2} min^{-1})
$\bar{r}$	Average reaction rate (g mol cm^{-2} min^{-1})
Sg	Specific surface area (m^2 g^{-1})
T	Temperature (K)
V_r	Reactor volume (cm^3)
v	Recorder chart velocity (cm min^{-1})
y_{H_2}	Reactant gas molar fraction (dimensionless)
X, Y	Potentiometric recorder coordinates (cm)
X_c	X coordinate value at complete conversion time (cm)
x	Conversion
z	Distance through which species are diffusing (cm)
ε	Porosity (dimensionless)
ϱ	Density of the reactant (g cm^{-3})
Φ	Modified Thiele modulus
τ	Necessary time to complete the reaction

Subscripts:

i	i component
0	initial value
en	entrance
ex	exit

1. Introduction

The reduction of iron oxides has been studied for many years and a very large number of experimental results have been reported [1–8]. However, the complexity of the system, combined with the fact that the reduction was carried out under different experimental conditions, has led to a wide variety of opinions about its mechanism.

Most reduction studies have been performed on pellets of dense haematite or magnetite using pure hydrogen or carbon monoxide as reducing agents. In recent years the interest in producing iron by direct reduction as an alternative to the blast-furnace has increased and some work has been done using CO/H_2 gas mixture [9, 10]. Generally speaking the results were correlated in terms of a model for a topochemical

*Research Fellow of the Consejo Nacional de Investigaciones Científicas y Técnicas, Buenos Aires, Argentina.
† Author to whom all correspondence should be addressed. *Present address*: POLISUR S.M. Casilla de Correo 651, (8000) Bahía Blanca, Argentina. Member of the Carrera de Investigador Científico of the Consejo Nacional de Investigaciones Científicas y Técnicas, Buenos Aires, Argentina.

0022–2461/88 $03.00 + .12

behaviour which assumes that the advance of the interfaces between iron, FeO_x, and Fe_3O_4 is linear with time. Most workers have found two different activation energy values ranging between 9 and 14 kcal mol^{-1} at temperatures lower than 833 K and 15 to 16 kcal mol^{-1} at higher temperatures.

The purpose of the present study was to measure the intrinsic kinetics of the reduction of the pure haematite by hydrogen, particularly in the temperature region where direct gas–solid reaction and diffusion of ions in the solid matrix seems to take place.

The thermodynamics of the reaction system under study is [11]

$$3Fe_2O_3 + H_2(G) \rightleftharpoons 2Fe_3O_4 + H_2O(G)$$

$$\Delta G^0 = 600 - 20.18\,T \quad (1)$$

$$Fe_3O_4 + H_2(G) \rightleftharpoons 3FeO + H_2O(G)$$

$$\Delta G^0 = 1450 - 16.58\,T \quad (2)$$

$$FeO + H_2(G) \rightleftharpoons Fe + H_2O(G)$$

$$\Delta G^0 = 3050 - 1.68\,T \quad (3)$$

$$Fe_3O_4 + 4H_2(G) \rightleftharpoons 3Fe + 4H_2O(G)$$

$$\Delta G^0 = 24\,800 - 21.62\,T \quad (4)$$

These reactions are apparently independent of pressure. As can be seen Reaction 1 is almost irreversible and Fe_2O_3 could be reduced even in the presence of a considerable amount of water in the gaseous phase. Reaction 2 does not occur if the reduction temperature is below 833 K. In order to accomplish the reactions under conditions of irreversibility, high hydrogen flows are advisable to sweep the water formed away from the reacting solid shell.

In view of the complex nature of the system, it was suitable to perform the reduction study under experimental conditions ensuring chemical control. These conditions could be reached using a fixed-bed reactor operating under differential conditions. The use of a differential reactor demands a very sensitive experimental technique.

In this work the kinetic study was carried out by measuring the hydrogen consumption through the analysis of the thermal conductivity change of the gaseous phase during the reaction. This technique has a sensitivity larger than other thermal analysis techniques such as DTA and TGA. The application of this method in the analysis of non-catalytic gas–solid reactions has been reported by Koussaev [12], but the appropriate treatment of the experimental results has been developed by Williams [13] and successfully employed in his kinetic study of the zinc dichromate reduction by hydrogen [14].

2. Experimental details

2.1. Materials

Pure powdered haematite (Fischer p.a.) was used. This material, conveniently characterized by X-ray diffraction, infra-red spectroscopy and chemical analysis, has proved to be pure α-Fe_2O_3.

The final reduction product was identified by X-ray diffraction as being metallic iron. The specific surface area of haematite, measured by the BET method using nitrogen adsorption was 17 m^2 g^{-1}. Porosimetry measurements on both initial and final solid reduction product were performed with an Aminco porosimeter. The gaseous reagents were high-purity hydrogen and nitrogen.

2.2. Reactor operation

Fig. 1 shows a schematic drawing of the experimental equipment. The haematite sample, contained in the stainless steel tube, was surrounded by an electric furnace whose temperature could be either kept constant, or controlled by a linear temperature controller.

In the isothermal operation, the inert nitrogen carrier gas was replaced by a H_2–N_2 reducing mixture when the required temperature was reached, and then the change in hydrogen concentration was monitored by the thermal conductivity detector and displayed on a recorder.

When the experiments with linear increase of temperature were carried out, the H_2–N_2 reducing mixture flowed through the reactor as soon as heating of the system started. Because the gas flow was constant, the change in hydrogen concentration was proportional to the rate of hydrogen consumption, or rate of iron oxide reduction.

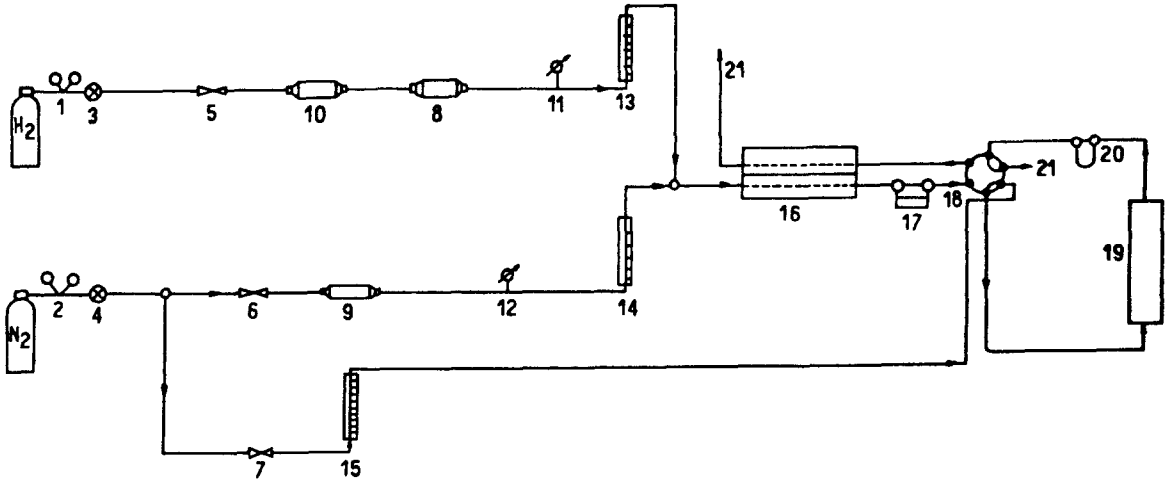

Figure 1 Flow sheet of the experimental equipment. 1, 2, Gas regulator; 3, 4, needle valves; 5–7, on-off valves; 8, 9, silica gel desiccant; 10, H_2 purifier; 11, 12 manometers; 13–15, flowmeters; 16, thermal conductivity cell; 17, H_2O saturater; 18, selective valve; 19, differential reactor; 20, desiccant; 21, exit.

The gas leaving the reactor passed through an absorption tube that removed the water produced by reduction. This trap may have produced axial dispersion of the gaseous phase. Care was taken to select an adequate water trap in order to avoid axial dispersion in the gaseous mixture before reaching the detection cell.

Customarily, about 0.3 g very fine powdered haematite (10^5 mm mean diameter of particle) was charged in the reactor, using a 1.45 to 2.50 10^{-3} gmol min^{-1} reducing gas flow.

3. Analysis of the experimental information

Fig. 2 shows a potentiometric record of the signal generated by a thermal conductivity cell for the time of reaction under isothermal conditions. The curve plotted is called the kinetic curve. Reactions represented by this type of curve are mentioned in the literature as "instantaneous germination" having their maximum velocity in the initial instant. For this kind of reaction the specific velocity, k_s, is a constant independent of the degree of conversion [15].

The coordinate Y (cm) is proportional to the potential difference ΔmV in the recorder equipment, and the X (cm) coordinate is proportional to the time (t). The kinetic curve is orginated by the signal variation with respect to the base line ($Y = 0$), corresponding to the continuous change of the thermal conductivity of the gaseous phase due to the hydrogen consumption by the reaction. The signal returns to the base line when the iron oxides are completely reacted.

The experimental information is interpreted in terms of Koussaev's procedure [12], which assumes that the relative variation of the molar fraction of the hydrogen in the measure branch of the detector with respect to the reference branch, is given by:

$$\frac{\Delta y_{H_2}}{y_{H_2}} = \frac{F_H/(F_H + F_N) - (F_H - F_R)/(F_H + F_N - F_R)}{F_H/(F_H + F_N)} \quad (5)$$

where F_H is the molar flow of hydrogen in the reference branch of the detector (gmol H_2 min^{-1}), F_N the molar flow of nitrogen in the reference branch of the detector (gmol N_2 min^{-1}), and F_R the molar flow of hydrogen which disappears by reaction (gmol H_2 min^{-1}).

Equation 5 may be rearranged into:

$$\frac{\Delta y_{H_2}}{y_{H_2}} = \frac{F_N F_R}{F_H(F_N + F_H - F_R)} \quad (6)$$

The response of the detector is, on the other hand, proportional to the left-hand side member of Equation 6.

$$\Delta \text{ mV} = f_{DT}\, \Delta y_{H_2}/y_{H_2} \quad (7)$$

f_{DT} being a constant factor whenever $\Delta y_{H_2}/y_{H_2} < 0.05$ [12] which means linear response behaviour. Recalling William's treatment [13, 14] one can write:

$$\Delta \text{ mV} = f_e\,(\text{mV cm}^{-1})\; Y\,(\text{cm}) \quad (8)$$

where Y is the height of the signal with respect to the base line and f_e is the recorded signal scale factor.

Bearing in mind the differential character of the reactor (see Appendix 2) one may consider in Equation 6 that $F_R \ll F_H + F_N$, then the molar flow of hydrogen disappearing by reaction may be written as follows.

$$F_R = \frac{F_H(F_H + F_N)\,\Delta \text{mV}}{F_N f_{DT}} \quad (9)$$

From this equation, Williams [13, 14] obtained (the intermediate steps are developed in Appendix 1) an expression of reaction rate:

$$r_M\,(\text{min}^{-1}) = \frac{v\,(\text{cm min}^{-1})\; Y\,(\text{cm})}{A\,(\text{cm}^2)} \quad (10)$$

where v is the recorder chart velocity, and A the area under kinetic curve. In a non catalytic gas–solid reaction, the reaction rate may be conveniently expressed as [13, 14]:

$$r_S\,(\text{g mol min}^{-1}\,\text{m}^{-2}) = \frac{r_M N_H}{S g_0} \quad (11)$$

N_H being the number of moles of hydrogen reacting with 1 g haematite. N_H may be calculated from the chemical analysis of the solid. In the present case $N_H = 1.87 \times 10^{-2}$ gmol H_2/g Fe_2O_3. Sg_0 is the specific surface area of the haematite.

By evaluating Equation 11 at the initial instant of the reaction, it results:

$$r_{S_0} = \frac{r_{M_0} N_H}{S g_0} \quad (12)$$

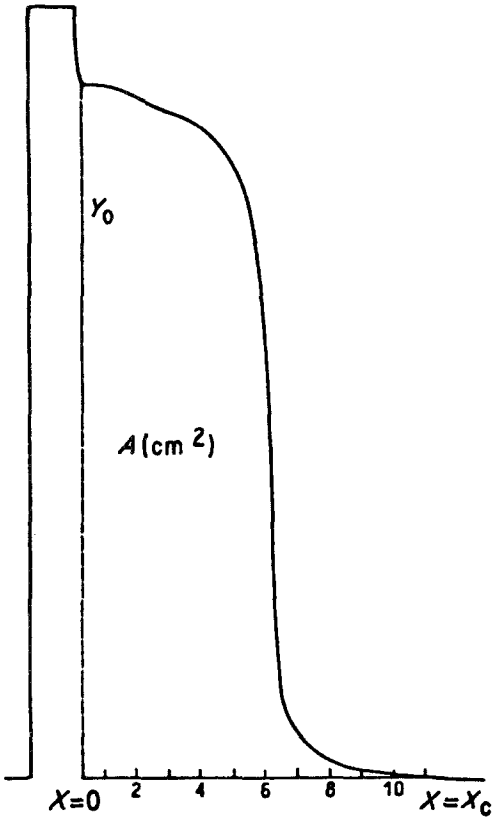

Figure 2 Ponteciometric plot of the signal from the thermal conductivity detector. $P_m = 0.3038$ g; $F_r = 1.45 \times 10^{-3}$ g mol min^{-1}; $y_{H_2} = 0.46$.

TABLE I

T (K)	F_T (10^3 gmol min^{-1})	$y_{H_2}{}_{en}$	$y_{H_2}{}_{ex}$	$\frac{\Delta y_{H_2}}{y_{H_2}}$	$\bar{y}_{H_2}$	y_{H_2O}	r_{Mo} (min^{-1})	r_{S_0} (10^5 gmol min^{-1} m^{-2})	r_{S_0}/y_{H_2} $\times 10^5$
968	1.45	0.463	0.447	0.034	0.455	0.016	0.032	3.52	7.60
968	1.45	0.257	0.250	0.027	0.253	0.007	0.017	1.87	7.27
968	2.29	0.635	0.614	0.033	0.624	0.015	0.042	4.62	7.27
968	2.29	0.385	0.381	0.010	0.383	0.004	0.025	2.75	7.14
978	2.29	0.110	0.108	0.018	0.109	0.009	0.010	1.10	10.00
978	1.45	0.257	0.249	0.031	0.253	0.008	0.026	2.86	11.10
978	1.45	0.460	0.444	0.034	0.452	0.016	0.044	4.84	10.52
978	2.29	0.600	0.583	0.028	0.591	0.017	0.061	6.71	11.18
1008	2.29	0.430	0.413	0.039	0.421	0.017	0.069	7.59	17.65
1008	1.45	0.430	0.419	0.025	0.424	0.011	0.071	7.81	18.16
1015.5	2.48	0.210	0.202	0.038	0.206	0.007	0.032	3.52	16.76
1018	2.48	0.100	0.096	0.040	0.098	0.003	0.017	1.87	18.70
1018	2.48	0.400	0.386	0.035	0.393	0.014	0.067	7.37	18.42
1018	2.49	0.580	0.562	0.031	0.572	0.018	0.096	10.56	18.20
1018	1.33	0.200	0.195	0.025	0.197	0.005	0.032	3.52	17.60
1045.5	2.48	0.428	0.410	0.042	0.419	0.018	0.076	8.36	19.53
1063	2.48	0.210	0.202	0.038	0.206	0.008	0.033	3.63	17.28

where r_{Mo} is calculated using the initial ordinate value Y_0 of the kinetic curve.

On the other hand, r_{S_0} may be written as:

$$r_{S_0} = k_s f(y_{H_2}) \quad (13)$$

As said before, in the type of reaction with instantaneous germination, k_s is a constant rate coefficient independent of the conversion of the solid, thus r_{S_0} will be constant all through the reaction.

4. Results and discussion

The isothermal reduction runs were performed covering the temperature range 968 to 1063 K and hydrogen partial pressure range 0.1 to 0.7 atm. Table I gives the results obtained; it may be observed that in all tests the ratio $\Delta y_{H_2}/y_{H_2}$ was less than 0.05, so that f_{DT} may be considered a constant factor.

The temperature-programmed reduction measurements were carried out at a temperature increase of 5° C min^{-1}, a reducing gas flow of 1.9×10^{-3} gmol min^{-1} and a hydrogen partial pressure of 0.58 atm.

Analysis of the TPR profile was performed as follows. Because the shape of the left side of the first peak (I) (Fig. 3) is experimentally determined, it serves for the construction of the total form of the peak with the aid of the "mirror method" in view of its symmetrical shape. Further peaks were obtained by subtracting peak I from the profile and so forth.

4.1. Porosimetry measurements

Porosimetry measurements were performed on both the initial (haematite) and the final product (metallic iron). Comparison of the two distributions indicated a substantial increase in porosity due to reduction as shown in Fig. 4.

4.2. Kinetic measurements

The purpose of these experiments was to measure the intrinsic kinetics by establishing both the hydrogen partial pressure, and the temperature dependence of the reaction rate.

4.2.1. Effect of hydrogen partial pressure

The influence of the hydrogen partial pressure on the reaction rate is illustrated in Fig. 5. As can be observed, the reduction rate is directly proportional to the hydrogen partial pressure throughout the entire pressure and temperature ranges. In fact, the plots

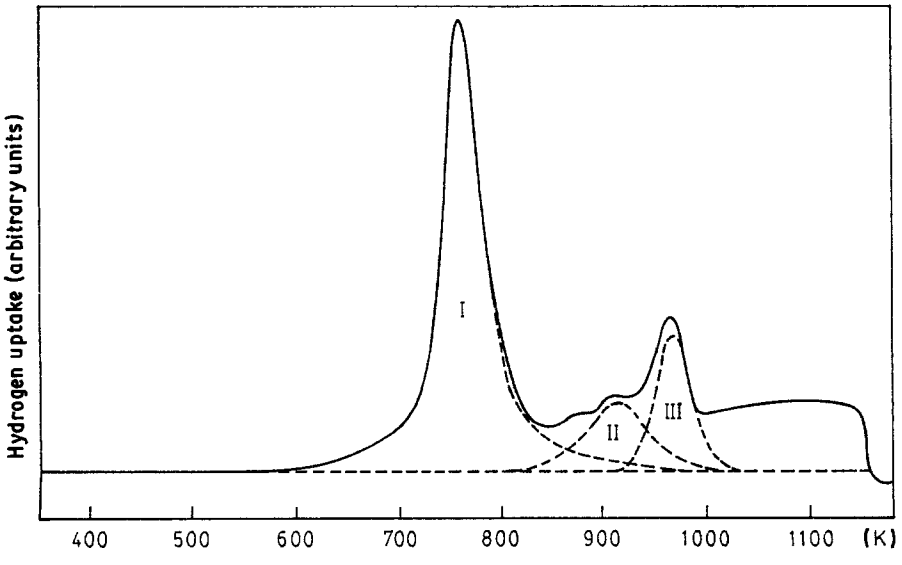

Figure 3 Temperature programmed reduction curve of Fe_2O_3. I, II, III: reduction steps.

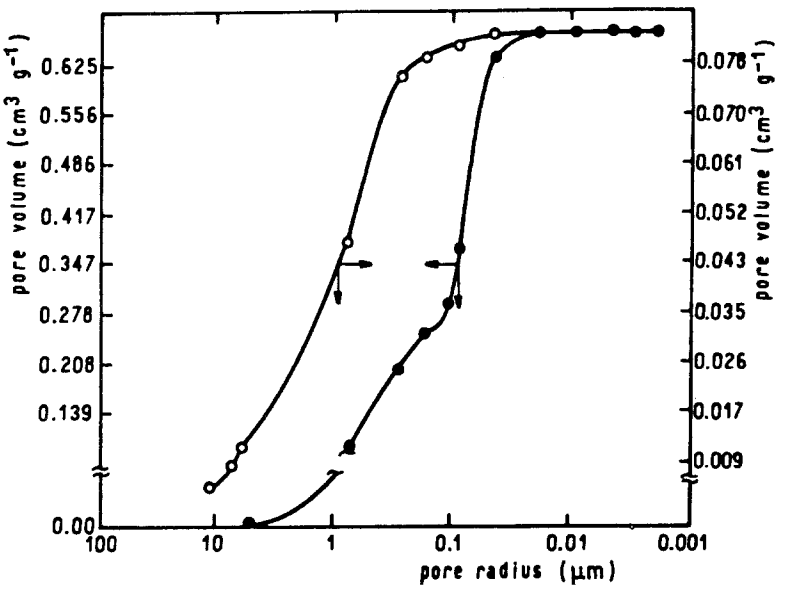

Figure 4 Porosimetric curves. ●, α-Fe_2O_3; ○, Fe.

show that the reduction of haematite is first order with respect to the hydrogen concentration. Such results may indicate the absence of diffusional effects, because a linear increase rate with hydrogen partial pressure would not occur if gas diffusion were rate controlling.

4.2.2. Effect of temperature

The effect of temperature on the reduction kinetics is shown in Fig. 6. The Arrhenius plot is obtained by representing the reaction rate constant (expressed as r_{S_0}/y_{H_2}) as a function of the inverse of absolute temperature.

The experimental points fall on two straight lines.

A sharp transition in the kinetic behaviour is observed in the temperature range 1008 to 1018 K. An activation energy of 40.2 $\pm$ 1.6 kcal gmol^{-1}, and a pre-exponential factor of 9.96 $\times$ 10^4 were obtained in the temperature region lower than 1008 K.

The experimental points above 1018 K exhibit considerable spread, for this reason the activation energy was not evaluated in this region.

Most authors found two different values for activation energy, but corresponding to the 823 to 843 K temperature range, it being largely demonstrated that wustite phase formation (unstable below 833 K) is responsible for this abrupt kinetic change.

This is not so in our case. In order to shed some light on this process a temperature-programmed reduction (TPR) was carried out. The TPR profile as shown in Fig. 3 provides a clear demonstration of the complex nature of the reaction involving several steps, allowing us to differentiate the individual reduction steps at the different temperatures. At first sight, four reduction peaks may be distinguished. Because of the natural line width of the peaks, some overlap is observed. From the deconvoluted TPR profile three well-defined steps of reduction, and a fourth flat contoured step may be observed. The integrated area under the TPR profile corresponds to the total number of moles of hydrogen used in the reaction:

$$Fe_2O_3 + 3H_2 \rightarrow 2Fe^0 + 3H_2O$$

The area under each individual peak represents the corresponding fraction of the total hydrogen consumption. On this basis it has been possible to propose the following sequence of reduction which is in agreement with the stoichiometry and the thermodynamic requirements

$$\left.\begin{aligned} Fe_2O_3 + \tfrac{1}{3}H_2 &\rightarrow \tfrac{2}{3}Fe_3O_4 + \tfrac{1}{3}H_2O \\ \tfrac{1}{3}Fe_3O_4 + \tfrac{4}{3}H_2 &\rightarrow \alpha\text{-}Fe^0 + \tfrac{4}{3}H_2O \end{aligned}\right\} \text{First step (Peak I)}$$

(670 to 825 K)

$$\tfrac{1}{3}Fe_3O_4 + \tfrac{1}{3}H_2 \rightarrow FeO + \tfrac{1}{3}H_2O \} \text{Second step (Peak II)}$$

(873 to 950 K)

$$\tfrac{1}{3}FeO + \tfrac{1}{3}H_2 \rightarrow \tfrac{1}{3}\gamma\text{-}Fe + \tfrac{1}{3}H_2O \} \text{Third step (Peak III)}$$

(950 to 1008 K)

$$\tfrac{2}{3}FeO + \tfrac{1}{3}H_2 \rightarrow \tfrac{2}{3}Fe^0 + \tfrac{2}{3}H_2O \} \text{Fourth step (Peak IV)}$$

(1008 to 1150 K)

Contrary to the isothermal reduction, characterized by an initial rate of considerable magnitude (often the

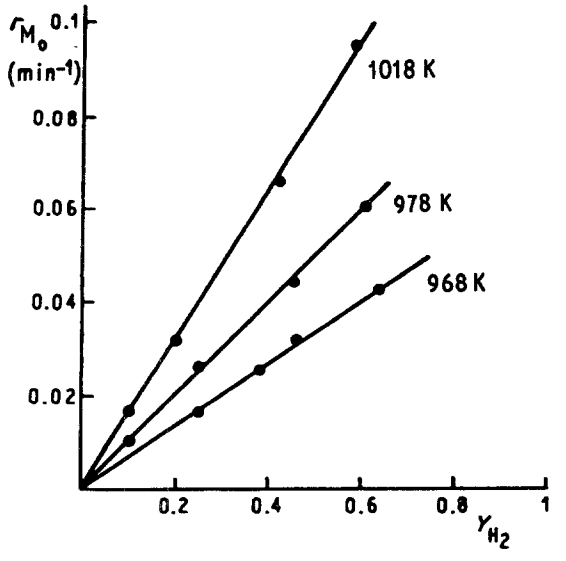

Figure 5 H_2 partial pressure influence on the haematite reduction rate.

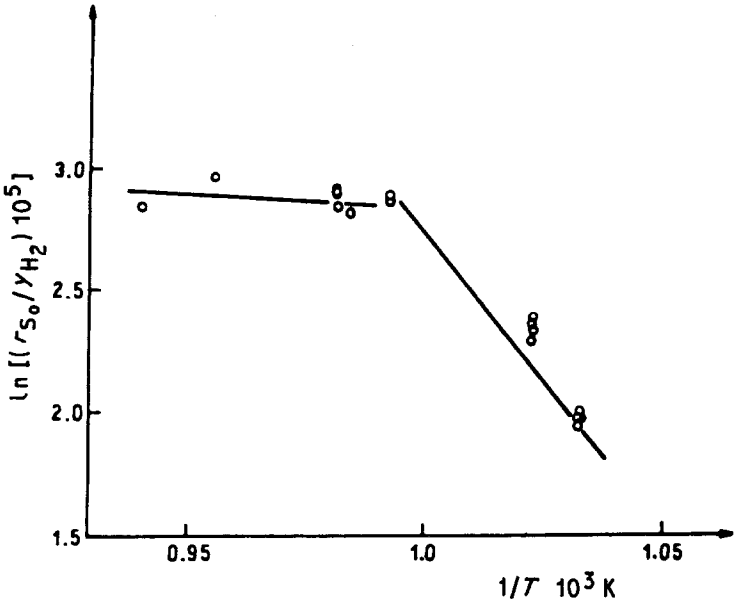

Figure 6 Temperature influence on the haematite reduction rate.

maximum value), the TPR profile reveals an initial induction period where the reaction is almost nil. This phenomenon is only observed under such conditions that the growth of nuclei at the oxide surface (germination) is slow enough to be recorded. This fact explains why most of the reported induction periods were observed at low temperatures [15].

The latent period is followed by a rugged acceleration of the reaction until the rate reaches its maximum value. The reduction of Fe_2O_3 to Fe_3O_4 and α-Fe is extremely rapid (Peak I) suggesting that an autocatalytic process takes place. The autocatalysis may be the result of the quite porous product formed during the haematite reduction which may accelerate the reduction to metal because of the higher surface area available for gas attack.

The diminishment of the TPR peak, despite the increasing reaction temperature, indicates that the conversion of Fe_3O_4 to FeO (Peak II) proceeds at much slower rate. The onset of FeO reduction is rapid (Peak III), only a part of the wustite phase being reduced in this step. The remaining oxide is completely reduced at a slower and almost constant rate beyond 1008 K (Peak IV).

The sudden change in the slope of the Arrhenius plot observed around 1008 K and the flatness of the TPR profile (constant hydrogen consumption) could indicate that the process is controlled by diffusion of the gaseous species. On the other hand, the first order kinetics observed over the entire range of hydrogen partial pressure and temperature, the small particle size of the solid and the increase of porosity observed in the completely reduced solid, induce us to discard gas diffusion as the controlling step. In fact, calculation of the diffusional effects under the operating conditions (see Appendix 3) demonstrates that they are negligible. The phenomenon observed beyond 1008 K could then indicate that the reduction of residual oxide is accomplished by a different process which is more sensitive to temperature that the direct gas–solid reaction, namely iron-ion migration into the solid phase.

Edstrom and Bitsianes [1] proposed that the reduction of haematite and magnetite results from the inward diffusion of iron ions in the solid phases. Edstrom [2] demonstrated that the mobility of iron ions in wustite varies over one hundred-fold between 973 and 1273 K. These facts suggest that the reduction of haematite to iron via magnetite and wustite primarily depends on the penetration and attack of the oxide phases by the reducing gas. Above 1008 K the oxygen lattice of wustite is completely destroyed, iron ions must move in order to form the metallic structure, and the process is controlled by the gas–solid reaction the rate of which is far exceeded by the rate of iron-ion mobility.

The retarded final reduction is mentioned by several authors; however, no one has reported two values of activation energy the temperature region beyond 833 K, corresponding to the different processes that evidently take place. The wide variety of opinion among authors about how the reduction of iron ores takes place is probably due to the differences in experimental techniques and iron ores. The great sensitivity of the experimental technique applied in the present work enables us to detect processes which are different in nature proceeding over the entire temperature range under study.

5. Conclusions

The reduction of powdered haematite was carried out in the temperature range 968 to 1063 K under different partial pressures of hydrogen. The great sensitivity of the experimental technique applied allowed us to detect two different processes taking place. One, occurring between 968 and approximately 1008 K, seemed to be chemically controlled, having an activation energy of $40.2 \pm 1.6\,\text{kcal mol}^{-1}$. The other, observed at temperatures beyond 1008 K, was a retarded reduction, indicating that direct gas–solid reaction and iron-ions diffusion mobility in the solid may be involved.

The results reported in the literature corresponding to temperatures higher than 833 K do not reveal the existence of two different processes. However, the comparatively low activation energy values found by

most workers may indicate that these values correspond to a sum of the processes mentioned above.

Acknowledgement

This study was supported by the Consejo Nacional de Investigaciones Científicas y Técnicas (Argentine).

Appendix 1

In Equation 9 the term $F_H(F_H + F_N)/F_N f_{DT}$ has a different value for each experiment, thus we can rewrite the equation as follows:

$$F_R = K\,\Delta\mathrm{mV} \tag{A1}$$

Bearing in mind Equation 8 and replacing it in Equation A1, it follows:

$$F_R = K'\,Y \tag{A2}$$

where $K' = Kfe$. The constant K' may be calculated for each experiment by integrating Equation A2 with respect to time:

$$\int_0^\tau F_R\,dt = K\int_0^\tau Y\,dt \tag{A3}$$

τ being the time necessary to complete the reaction. The integral of the left-hand side of Equation A3 may be obtained as follows:

$$\int_0^\tau F_R\,dt = N_H\,m \tag{A4}$$

In addition, the right-hand side of Equation A3 may be calculated as:

$$\int_0^\tau Y\,dt = v^{-1}\int_0^{X_c} Y\,dX = A/v \tag{A5}$$

by calculating K' using Equations A3 to A5 and replacing it in Equation A2 it follows:

$$F_H = N_H m v Y(X)/A \tag{A6}$$

By writing the reaction rate in terms of r_M (time^{-1}), and as $X = tv$, it results:

$$r_M = F_H/(N_H m) = v\,Y(t)/A \tag{A7}$$

In each experimental run, the $r_M(t)$ function may be easily calculated, avoiding the periodical calibration of the thermal conductivity detector.

Appendix 2. Differential reactor condition

The mass balance of the reference component i in a flow reactor may be written as follows:

$$F_v C_{i0}\,dx_i = r_i(x_i)\,V_r \tag{A8}$$

By integrating Equation A8 we obtain

$$\frac{V_r}{F_v C_{i0}} = \int_0^{x_i}\frac{dx_i}{r_i(x_i)} \tag{A9}$$

Because composition changes from point to point, r_i varies to some extent along the reactor, and the measured value of the reaction rate is an average value $\bar{r}_i$ integrated for the whole reactor, and can be written by solving Equation A9 as follows:

$$\bar{r}_i = \frac{F_V C_{i0}}{V_r}\,x_i \tag{A10}$$

When the differential method is used to establish the rate equation the measured reaction rate is usually correlated with the arithmetic average composition between the entrance and the exit of the reactor [16]. This condition may be written as $r_i = r_i(\bar{y}_i)$ then the differential reactor condition is verified when,

$$\bar{r}_i(x) = r_i(\bar{y}_i) \tag{A11}$$

that is when the average reaction rate is equal to the true local reaction $r_i(\bar{y}_i)$ at the point where composition is just the arithmetic average value: $\bar{y}_i = 0.5\,(y_{en} + y_{ex})$. It will be demonstrated that the experiments of the present work verify Equation A11.

By replacing Equation A9 in Equation A10 and considering a first-order kinetics, we obtain:

$$\bar{r}_i(x_i) = \frac{x_i}{\displaystyle\int_0^{x_i}\frac{dx_i}{k_s C_{i0}(x_i - x_{i0})}} \tag{A12}$$

By solving Equation A12 it results:

$$\bar{r}_i(x_i) = \frac{x_i k_s C_{i0}}{\ln(1/1 - x_i)} \tag{A13}$$

On the other hand, for first-order kinetics $r(\bar{y}_i)$ may be written as follows:

$$r_i(\bar{y}_i) = k_s\left(\frac{y_{en} + y_{ex}}{2}\right)$$

Table AI shows $\bar{r}(x_i)$ and $r(\bar{y}_i)$ values for the reduction of haematite with hydrogen under experimental conditions. As may be seen, the very good agreement demonstrates the validity of the differential reactor under the chemical controlling hypothesis in the experimental kinetics runs.

TABLE AI

T (K)	$\bar{r}_{S_0}(x)$ (10^5 gmol min^{-1} m^{-2})	$r_{S_0}(\bar{y}_{H_2})$ (10^5 gmol min^{-1} m^{-2})
968	3.458	3.459
968	1.849	1.840
968	4.543	4.539
968	2.736	2.735
978	1.085	1.090
978	2.815	2.815
978	4.757	4.755
978	6.615	6.607
1008	7.441	7.439
1008	7.711	7.709
1015.5	3.452	3.452
1018	1.832	1.832
1018	7.240	7.239
1018	10.405	10.410
1018	3.471	3.467
1045.5	8.183	8.183
1063	3.560	3.559

Appendix 3. Verification of chemical controlling hypothesis

In order to verify that the kinetics measurements are carried out under chemical controlling conditions it is necessary to demonstrate the absence of both external and internal concentration gradients due to diffusional effects.

(a) External concentration gradient

The molar flow of hydrogen from the bulk gaseous phase to the solid particle surface under steady state conditions is equal to the chemical reaction rate:

$$r_s = -D_{H_2-N_2} \left.\frac{dC_{H_2}}{dz}\right|_{sup} \quad \text{(A14)}$$

By integrating through the thickness of the gaseous boundary layer

$$\Delta C_{H_2} = r_s \frac{L}{D_{H_2-N_2}} \quad \text{(A15)}$$

or by assuming ideal behaviour

$$\Delta y_{H_2} = r_s \left(\frac{L}{D_{H_2-N_2}}\right)\left(\frac{R_g T}{p}\right) \quad \text{(A16)}$$

Because L cannot be higher than the particle radius, we take this value as the upper confidence limit, thus:

$$\Delta y_{H_2} = r_s \frac{d_p}{2D_{H_2-N_2}} \frac{R_g T}{P} \quad \text{(A17)}$$

Δy_{H_2} is calculated for the reaction of reduction of haematite by hydrogen at the highest temperature which the kinetics measurements are carried out (1063 K). Then, $r_s = 3.63 \times 10^{-5}$ gmol min^{-1} m^{-2}, $d_p = 0.010$ cm, and $D_{H_2-N_2} = 5.68$ cm^2 sec^{-1} is calculated by using the Chapman–Enskog equation [17]. By introducing the corresponding values in Equation A17 we obtain: $\Delta y_{H_2} = 4.64 \times 10^{-6}$.

The diminution undergone by the hydrogen concentration through the gaseous boundary layer is negligible and the external diffusional effects may also be considered negligible.

(b) Internal diffusional effects

The internal diffusional effects are evaluated using the well known criterion developed by Weiz and Prater [18], which states that a first-order reaction system can be considered safe from internal diffusional effects (i.e. effectiveness factor $\eta = 1$) when the following conditions are achieved:

$$\Phi = \frac{R^2}{D_{eff}} \frac{r_{V_0}}{C_i} \leqslant 1 \quad \text{(A18)}$$

where the factor Φ is a modified Thiele modulus $h = R(k C_i^{n-1}/D_{eff})^{1/2}$ and is a function of "observable" variables, and r_{V_0} is the reaction rate per unit of volume of reactant solid and is estimated from the experimental r_{S_0} value as follows:

$$r_{V_0} = r_S S g \varrho \ (\text{g mol cm}^{-3} \text{ min}^{-1})$$

The effective diffusivity, D_{eff}, may be related to the molecular diffusivity as follows [19]

$$D_{eff} = D_{H_2-N_2} \frac{2\varepsilon}{(3 - \varepsilon)}$$

where ε is the porosity and ϱ is the true density of the reactant solid, obtained from porosimetric measurements ($\varepsilon = 0.71$, $\varrho = 2.45$ g cm^{-3}). By assuming ideal behaviour for the gaseous reactant, the molar concentration C_i is expressed as $p/R_g T$.

Calculating the factor, Φ, at the highest temperature at which kinetics measurements were carried out (1063 K) the value $\Phi = 7.58 \times 10^{-5}$ is obtained. This result indicates that the internal diffusional effects are also negligible.

References

1. O. EDSTROM and G. BITSIANES, *AIME Trans.* **203** (1955) 760.
2. J. O. EDSTROM, *J. Iron Steel Inst.* **175** (1953) 289.
3. W. M. McKEWAN, *Trans. Met. Soc. AIME* **212** (1958) 791.
4. J. M. QUETS, M. E. WADSWORTH and J. R. LEWIS, *Trans. Met. Soc. AIME* **218** (1960) 545.
5. N. A. WARNER, *ibid.* **230** (1964) 163.
6. N. J. THEMELIS and W. H. GAUVIN, *ibid.* **227** (1963) 290.
7. N. B. GRAY and J. HENDERSON, *ibid.* **236** (1966) 1213.
8. R. G. OLSSON and W. M. McKEWAN, *ibid.* **236** (1966) 1518.
9. R. HUGHES, E. K. T. KAM and H. MOGADAM ZADEH, 2nd European Symposium on Thermal Analysis (1981) 455–9, Aberdeen, UK.
10. E. K. T. KAM and R. HUGHES, *Trans I. Chem E* **59** (1981) 196.
11. A. K. BISWAS and G. R. BASHFORTH, "The Physical Chemistry of Metallurgical Processes" (Chapman and Hall, London, 1962) p. 236.
12. YU. I. KOUSSAEV and YU. V. TZOETKOV, "Metallurgia Tzoetnichi Reckich Metallov" (IZD "Navak", Moscow, 1967) p. 73.
13. R. J. J. WILLIAMS, Thesis Doctoral, Univ. Nac. de La Plata (1972).
14. R. J. J. WILLIAMS and R. E. CUNNINGHAM, *Rev. Latinoam. Ing. Quím. Quím. Apl.* **3** (1973) 65.
15. B. DELMON, "Introduction a la Cinetique Hetérogene" (Technip, Paris, 1969).
16. H. A. MASSALDI and J. A. MAYMÓ, *J. Catal.* **14** (1969) 61.
17. J. O. HIRSCHFELDER, C. F. CURTISS and R. B. BIRD, "Molecular Theory of Gases and Liquids" (Wiley, New York, 1954) p. 539.
18. P. B. WEISZ and C. D. PRATER, *Adv. Catal.* **6** (1954) 143.
19. R. E. CUNNINGHAM and R. J. J. WILLIAMS, "Diffusion in Gases and Porous Media" (Plenum, New York and London, 1980) p. 134.

Received 13 November 1984
and accepted 15 January 1987